FWI VELOCITY AND IMAGING: A CASE STUDY IN THE JOHAN CASTBERG AREA

N. Salaun[1], M. Reinier[1], I. Espin[1], G. Gigou[1]

[1] CGG

Summary

The Greater Castberg survey was acquired in 2019 using a source-over-spread acquisition design with an additional source at the front of the streamers, towed by the receiver boat, to permit recording of longer offsets. Starting from an initial anisotropic model, time-lag full waveform inversion (TLFWI) was used to compute a 13 Hz velocity model over the 5000 km2 area, which led to a much improved migration image (e.g., better imaged reservoir flat spots). When pushing the inversion frequency up to 90 Hz, the resultant TLFWI velocity model enabled more detailed delineation of reservoir boundaries compared to the migration image. Furthermore, the FWI Image as an alternative view of the FWI velocity model, provided access to new reflectivity information, overcoming some limitations of current migration tools. The use of the full wavefield, including refraction, reflection of primary, multiple and ghost, greatly enhanced image without needing the complex data pre-processing required by conventional imaging. In the context of thick gas clouds, this new imaging technique provided accurate sub-gas reflectivity, which effectively enhanced event continuity compared to reverse time migration (RTM) results.

FWI velocity and imaging: A case study in the Johan Castberg area

Introduction
The Johan Castberg field, located in the Barents Sea, is composed of several recent oil discoveries which can be detected via their flat spot signatures. Contours of these flat spots have been improved by several seismic acquisition and processing campaigns designed to simplify the interpreters' task of delimiting the various blocks and possible fluid connections among them. The most recent survey was acquired in 2019 over a large area of 5000 km^2, using a dual azimuth source-over-spread acquisition design. This novel acquisition method has proven its great potential in producing high resolution imaging at all depths in this region (Dhelie et al., 2018) due to its naturally small bin size, precious zero-offset data and high near-offset fold.

Despite the high quality of the new recorded data, intensive processing efforts are still needed to obtain clean primary reflections for input to migration. However, this step suppresses a large amount of valuable information meaning that the densely-sampled full wavefield recorded by this acquisition cannot be fully utilized to predict the reflectivity. Full waveform inversion (FWI) is a natural way to use the full-wavefield data but is mostly used to derive the migration velocity. Zhang et al. (2020) recently proposed a modified FWI workflow – FWI Imaging – to directly output reflectivity images instead of the velocity. Using the Johan Castberg data, this paper demonstrates the interpretation benefit of FWI velocity and reflectivity due to the use of the full wavefield data including refraction, primary, multiple and ghost energy and the least-squares data fitting. More detail analysis on acquisition impact for FWI Imaging is discussed by Kerrison et al ([2021] Impact of streamer acquisition geometry on FWI Imaging, *submitted for 83rd EAGE Conference and Exhibition, Expanded Abstracts*).

From high resolution velocity to reflectivity
In addition to five "top" sources located over the streamers, the 2019 source-over-spread acquisition added a front source, towed by the receiver boat, to permit recording of long offset data up to 8 km. Long-offset data are very important for improving the velocity model building (VMB) and hence the accuracy of the imaging. In our workflow, long-offset data were used to run diving wave FWI while the dense top sources provided detailed residual moveout (RMO) information for tomography (Salaun et al., 2020). Starting from this advanced initial model, both front and top source data were jointly used in the final FWI. The combination of the two, allows matching of long offset diving wave information with the reflections, generating a robust velocity update for the shallow section, which is key to accurately modeling multiple reflection energy from the shallow generators. Use of the unmuted full trace length, containing deep reflections, allows updates to velocity deeper than the diving wave penetration (about 1.5 km on this survey). Dense sampling from the five top sources adds detail and mitigates acquisition footprint artifacts when increasing the maximum FWI frequency. To enable use of the full recorded information inside the inversion, first, the anisotropic epsilon parameter was inverted using a joint reflection and first break tomography (Allemand et al., 2020) to reconcile horizontal velocity derived from the diving waves with the vertical velocity derived from the reflected waves. Second, cycle-skipping and amplitude-discrepancy between synthetic and recorded seismic data were mitigated through time-lag FWI (TLFWI) that uses a kinematics-only cost function (Zhang et al., 2018). An accurate velocity field is crucial to ensure the proper migration of pre-processed seismic data, which is often the top criterion to judge its quality. However, the velocity model itself can also be a source of important information for direct reservoir interpretation (Schultz, 1988). On Figure 1, the flat spot is easily identified on the migration image due to improved migration velocity; nevertheless, it is still difficult, from this single image, to assess the compartments filled by hydrocarbons and their limits. Having access to both the migration image and a highly detailed velocity model over an entire 5000 km^2 area gives more confidence to interpreters.

The TLFWI maximum frequency can be increased to provide augmented benefits for direct interpretation. Figure 2b shows how a depth slice through a 90 Hz velocity field can accurately delineate the limit of the gas-oil contact, which is difficult to track on migration images. To view the velocity field in a way consistent with conventional migration images, Zhang et al., (2020) proposed a modified FWI workflow – FWI Imaging – to directly output reflectivity image:

$$\frac{\partial I}{\partial n} \approx \rho \left(\frac{\partial v}{\partial x} \sin \theta \cos \varphi + \frac{\partial v}{\partial y} \sin \theta \sin \varphi + \frac{\partial v}{\partial z} \cos \theta \right), \tag{1}$$

where the impedance is the multiplication of density (assumed constant or slowly varying here) and velocity, $I = \rho v$, and θ and φ are dip and azimuth angles of the normal vector to the subsurface reflectors, which can be obtained by automatically scanning through the velocity model.

The FWI Image contains information from the full wavefield data and also benefits from the least-squares data fitting process inherent to FWI. When compared with Kirchhoff PSDM (Figure 2d), migrated using effectively the same velocity model, the FWI Image (Figure 2e) shows sharper fault and structure termination (Figures 2d and 2e). We note that the Kirchhoff PSDM had gone through heavy preprocessing including 3D deghosting and 3D demultiple. Nevertheless, the Kirchhoff PSDM image suffers from a sub-optimal signal-to-noise ratio and recovers less reflectivity details than the FWI Image.
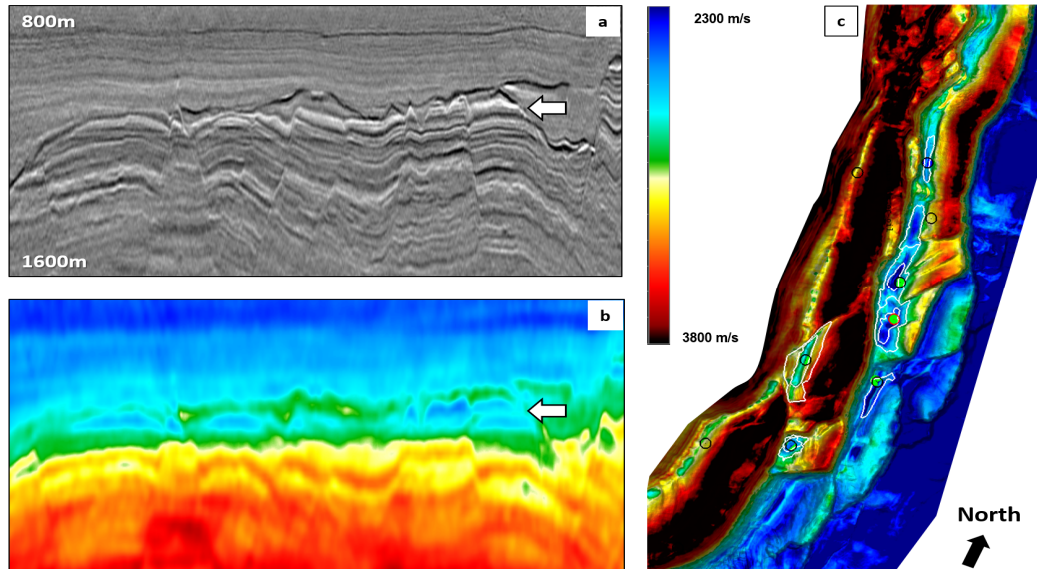

Figure 1: a) shows a cross section going through several known reservoirs. A flat spot is easily traceable along the faulted block, indicating the potential presence of hydrocarbons. From this single image however, it is difficult to fully delineate the reservoir, the addition of a detailed velocity field (b) is a real benefit to interpreters. Low velocity packages can be spotted indicating the limits of several known reservoirs. Superimposed flat spot limits, highlighted by white arrow, are now clear. When extracting velocity along a target horizon, it is possible to map all these fields (c). Blue to dark blue low velocity compartments can be observed on this velocity extraction, which fully correlate with presence of known discovery wells.

Sub-gas imaging
Compared to migration of primary reflections, FWI Imaging benefits from the additional information provided by refractions, multiple and ghost reflections, which is essential to image below complex geological features such as salt or gas clouds (Huang et al., 2021; personal communication). South of the Johan Castberg fields is a new reservoir recently discovered below thick gas clouds. With layered gas bodies reaching up to 300 m in vertical thickness, the uncertain image of the area earned it the name of *Takehavet*, "the ocean of mist". In this area, TLFWI was performed using a similar initial model and workflow but also including a Q factor model, computed by a diving-wave-only Q-FWI (Wang et al, 2018). The resulting Q-FWI Image at 40 Hz was then compared to Q-Kirchhoff PSDM and Q-reverse time migration (RTM) (Figure 3). The benefits of Q-RTM (Figure 3c) over Kirchhoff Q-PSDM (Figure 3b) are obvious due to its ability to handling large velocity anomalies. Compared to Q-RTM, the Q-FWI Image (Figure 3d) gave more balanced amplitudes, better sub-gas event continuity and sharper delineation of faults because of the use of full-wavefield data and least-squares data fitting.

Traditionally, data interpolation/ regularization has to be used to fill in acquisition holes to avoid migration footprints/ artifacts. However, this process can easily damage highly-diffracted events that often have weak amplitudes and high dips in the time domain. FWI Imaging, on the other hand,

experiences much less footprint issues because of the additional illumination from multiples and illumination compensation from least-squares data fitting and thus enhances the lateral resolution, which is critical for shallow hazard imaging (Figure 4). From the velocity field, it is also possible to use the horizontal components of the velocity gradient to obtain lateral reflectivity:

$$\sqrt{(\partial v/\partial x)^2 + (\partial v/\partial y)^2}, \qquad (2)$$

which highlights the edges of structures and fault networks.
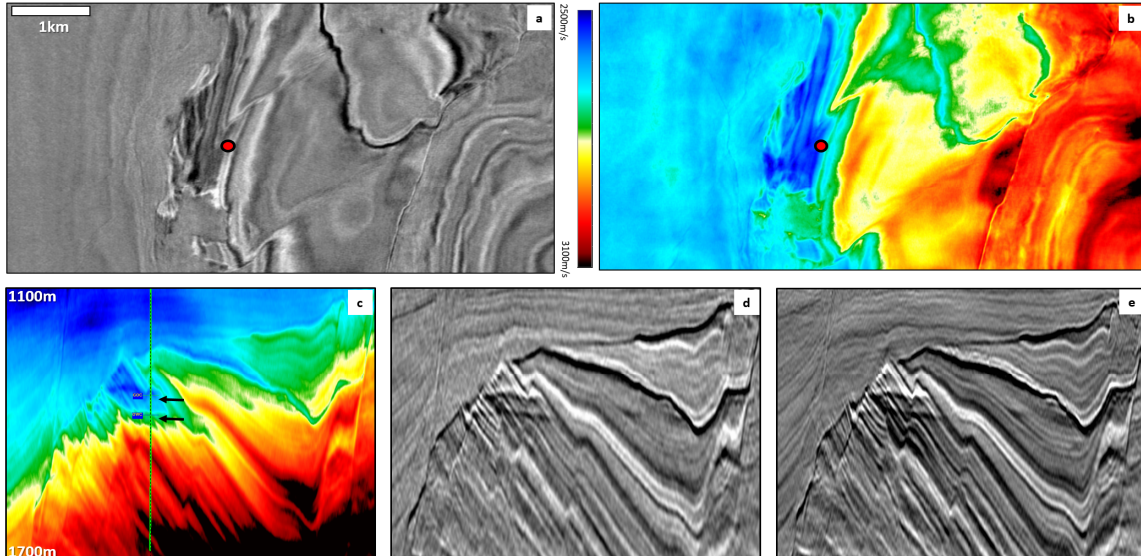

Figure 2: Panels (a) and (b) show PSDM and velocity depth slice at the gas-oil contact. On the 90 Hz TLFWI velocity model, the hydrocarbon area is highlighted by the slow velocity (blue) and edges of this region can be easily tracked to define the limits of the reservoir, which is more difficult on the migration image. Such high-resolution velocity models thus help in refining the reservoir volume. Panel (c) shows a cross-section of the velocity field at the well location, where both oil-water and gas-oil contacts are visible (black arrows), matching known well information. Reflectivity obtained by TLFWI (e) is compared to PSDM (d). The FWI Image shows higher resolution, improved signal-to-noise ratio and sharper events.
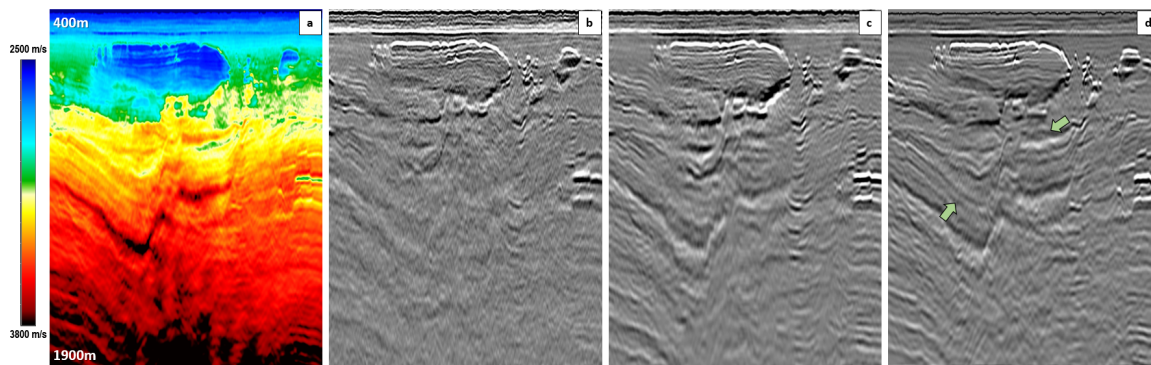

Figure 3: 40 Hz Q-TLFWI velocity model (a) was used to obtain: Q-KPSDM image (b), Q-RTM image (c) and Q-FWI Image (d) along a crossline section through a large gas cloud. Improvements from Q-KPSDM to Q-RTM are evident and expected for complex geological features such as gas; further improvements can be observed from Q-RTM to Q-FWI Image. Green arrows indicate areas where event continuity is well resolved, along with faults allowing the gas to leak upwards. The FWI Image is more interpretable below the gas, reducing uncertainty for interpreters.

Discussion and conclusion

Tarantola's (1986) prediction of using the products of inverse methods instead of migrating pre-processed seismic data has recently started to be practical (Kalinicheva et al., 2020; Zhang et al., 2020).

Indeed, avoiding the complex denoising and wavefield separation steps needed to isolate primary reflection energy, greatly simplifies the imaging sequence. The presented TLFWI Imaging examples on latest densely sampled long offset source-over-streamer acquisition show the improved imaging quality compared to the current industry standard, especially below complex gas clouds where signal quality is poor. The associated high-resolution velocity model can also be used to facilitate detail reservoir interpretation work.

However, despite the much-reduced steps in FWI imaging workflow, it has not yet become a fully automated process that does not require any human supervision The two main challenges are (1) adequate data quality, i.e. the requirement of long offset, well sampled data, with strong low frequency content, and (2) a sufficiently accurate initial anisotropic model to avoid cycle skipping and reasonable tie with the well information. In addition, the computational effort increases exponentially as we pursuit higher frequency for final products. With the continuous evolution on data acquisition, research, and computation technology, we shall see the quality and turnaround of FWI imaging continues to improve in near future.
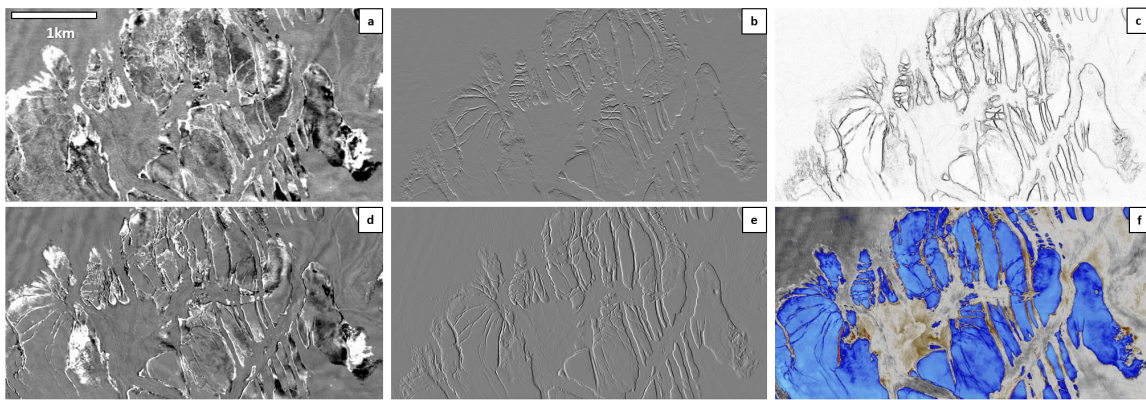

Figure 4: *Depth slice of Q-FWI Image (d) shows sharper gas package when compared to Q-KPSDM (a). By displaying lateral derivatives of the velocity (f) either along the x (e) or y (b), lateral reflectivity can be estimated for any azimuth. Panel c shows the horizontal derivative norm, which highlights the edge of structures. This dip image provides additional information to seismic reflection imaging and can be used as complementary information for shallow hazard surveys.*

Acknowledgements

References

Allemand, T., Sedova, A., Lambaré, G., Grenié, D. and Guillaume, P. [2020] Full Waveform Inversion in an Anisotropic Earth: A Practical Workflow. *82nd EAGE Conference and Exhibition*

Dhelie, P. E., Danielsen, V., Lie, J. E., Evensen, A. K., Wright, A., Salaun, N., Henin, G., Vinje, V. and Camerer, A. [2018] Improving seismic imaging in the Barents Sea by source-over-cable acquisition. SEG Technical Program Expanded Abstracts, 71-75

Kalinicheva, T., Warner, M. and Mancini, F. [2020] Full-bandwidth FWI. *82nd EAGE Conference and Exhibition*

Salaun, N., Reinier, M., Henin, G., Gigou, G. and Wright, A. [2020] Capturing the Value of Source-Over-Streamer Acquisition for Velocity Model Building at Barents Sea. *82nd EAGE Conference and Exhibition*

Schultz, P. [1998] The seismic velocity model as an interpretation asset. SEG distinguished instructor series, volume 2.

Tarantola, A. [1986] A strategy for nonlinear elastic inversion of seismic reflection data. Geophysics, **51**(10), 1893-1903.

Wang, M., Xie, Y., Xiao, B., Ratcliffe, A. and Latter, T. [2018] Visco-acoustic full-waveform inversion in the presence of complex gas clouds. SEG Technical Program Expanded Abstracts, 5516-5520

Zhang, Z., J. Mei, F. Lin, R. Huang, and Wang, P. [2018] Correcting for salt misinterpretation with full-waveform inversion. SEG Technical Program Expanded Abstracts, 1143–1147.

Zhang, Z., Wu, Z., Wei, Z., Mei, J., Huang, R. and Wang, P. [2020] FWI Imaging: Full-wavefield imaging through full-waveform inversion. SEG Technical Program Expanded Abstracts, 656-660